Journal of Structural Geology 31 (2009) 996–1011

Contents lists available at ScienceDirect

Journal of Structural Geology

journal homepage: www.elsevier.com/locate/jsg

Steeply-dipping extension fractures in the Newark basin, New Jersey

Gregory C. Herman*

N.J. Geological Survey, 29 Arctic Parkway, P.O. Box 427, Trenton, NJ 08625, USA

ARTICLE INFO

Article history:
Received 27 March 2007
Received in revised form
16 July 2008
Accepted 16 October 2008
Available online 29 October 2008

Keywords:
Newark basin
Mesozoic
Fractures
Joints
Veins
Extension
Tectonic

ABSTRACT

Late Triassic and Early Jurassic bedrock in the Newark basin is pervasively fractured as a result of Mesozoic rifting of the east–central North American continental margin. Tectonic rifting imparted systematic sets of steeply-dipping, en échelon, Mode I, extension fractures in basin strata including ordinary joints and veins. These fractures are arranged in transitional-tensional arrays resembling normal dip-slip shear zones. They contributed to crustal stretching, sagging, and eventual faulting of basin rift deposits. Extension fractures display progressive linkage and spatial clustering that probably controlled incipient fault growth. They cluster into three prominent strike groups correlated to early, intermediate, and late-stage tectonic events reflecting about 50– 60° of counterclockwise rotation of incremental stretching directions. Finite strain analyses show that extension fractures allowed the stretching of basin strata by a few percent, and these fractures impart stratigraphic dips up to a few degrees in directions opposing fracture dips. Fracture groups display three-dimensional spatial variability but consistent geometric relations. Younger fractures locally cut across and terminate against older fractures having more complex vein-cement morphologies and bed-normal folds from stratigraphic compaction. A fourth, youngest group of extension fractures occur sporadically and strike about E–W in obliquely inverted crustal blocks. A geometric analysis of overlapping fracture sets shows how fracture groups result from incremental rotation of an extending tectonic plate, and that old fractures can reactivate with oblique slip components in the contemporary, compressive stress regime.

1. Introduction

Steeply-dipping (>60°) to vertical extension fractures, including common joints, are ubiquitous in Early Mesozoic strata in the Newark basin. This article examines the morphology, mineralogy, and spatial distribution of these fractures in outcrop and the shallow subsurface in the New Jersey part of the basin. It demonstrates that steeply- dipping joints are primary structures developed throughout the basin's history, resulting in stretching, sagging, and eventual faulting of accumulating crustal deposits in the rift basin. Fracture characteristics reflect early Mesozoic tectonic evolution of the basin, portrayed here to stem from systematic, basin-wide stress changes on the developing continental margin.

Recent subsurface mapping using a digital optical televiewer in bedrock water wells has provided unprecedented access to the three-dimensional geometry and spatial distribution of these fracture systems and corroborates structural observations and measurements made in outcrop. A brief review of the geological setting precedes the discussion aimed at defining, classifying, and describing the fractures and their tectonic implications. Their physical properties are characterized using outcrop and hand sample relationships, microscopic petrography, and regional maps that emphasize fracture geometry and the spatial distribution of fracture sets. Coverage of other fracture systems dipping at gentle- to moderate angles and stemming from post-rifting tectonic compression and inversion, exhumation, erosion, glacial rebound, and weathering is beyond the scope of this paper.

2. Geological setting

The Newark basin is one of a series of tectonic rift basins of Mesozoic age formed on the eastern North American plate margin during the breakup of the supercontinent Pangea preceding formation of the Atlantic Ocean basin. It covers about 7500 km^2 and extends from southern New York across New Jersey and into southeastern Pennsylvania (Fig. 1). The basin is filled with Upper Triassic to Lower Jurassic sedimentary and igneous bedrock that is fractured, faulted, tilted, and locally folded (see summaries in Schlische, 1992, 2003; Olsen et al., 1996a).

Various tectonic models invoking multiple phases of 'rifting', 'shifting', and 'drifting' have been proposed to account for the

* Fax: +1 609 633 1004.
E-mail address: greg.herman@dep.state.nj.us

0191-8141/$ – see front matter © 2008 Elsevier Ltd. All rights reserved.
doi:10.1016/j.jsg.2008.10.008

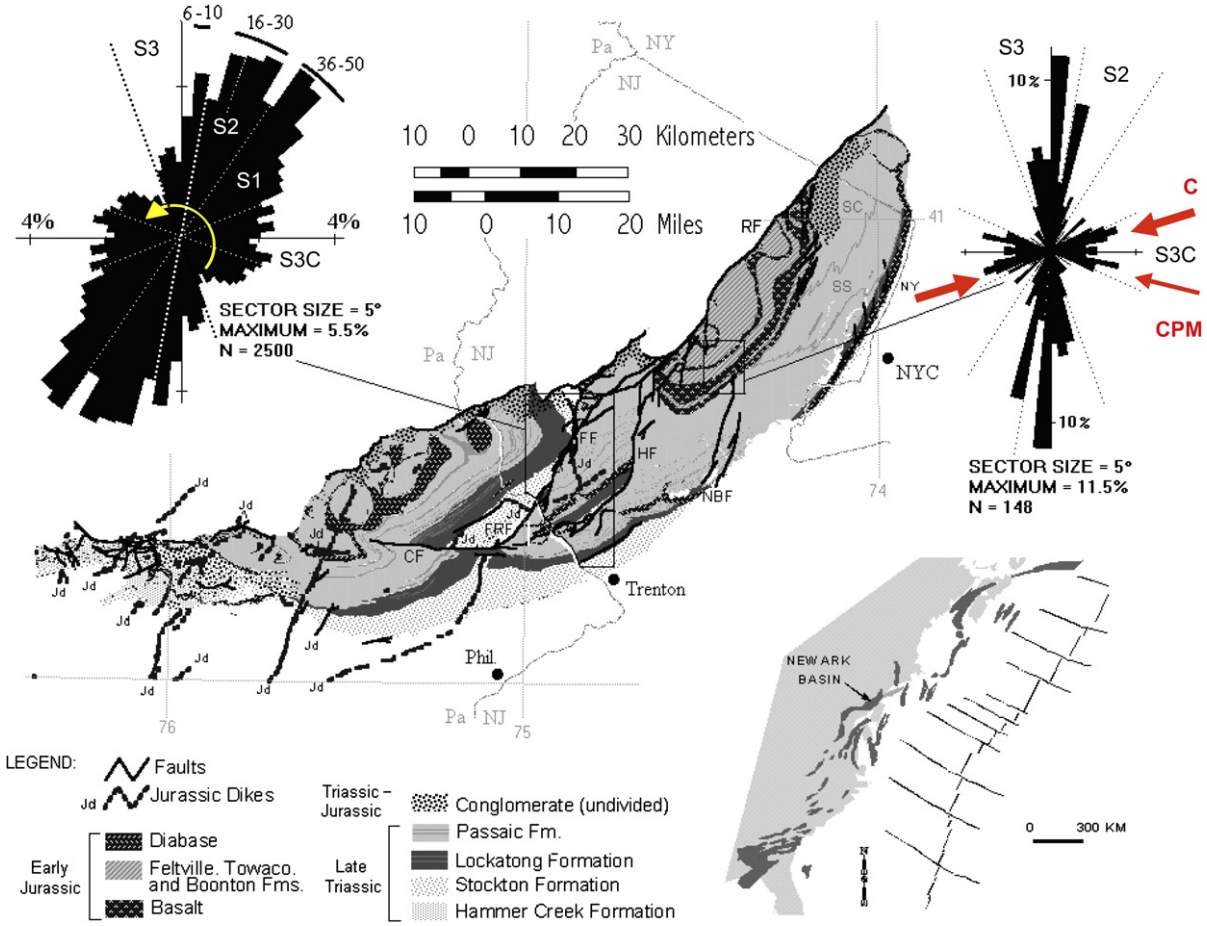

Fig. 1. Bedrock geology of the Newark basin compiled from geographic information system coverage for New Jersey (NJ Geological Survey, 2000), New York (http://www.nysm.nysed.gov/data/lhud_bedr1a.zip), and Pennsylvania (http://www.dcnr.state.pa.us/topogeo/map1/bedma.htm). Left histogram shows planar strike for 2500 sets of steeply-dipping extension fractures measured in ~1300 outcrops of Late Triassic sedimentary bedrock in six, 7-1/2′ quadrangles in the center of the basin. Extension fractures in Late Triassic rocks mostly strike between N16° and N50°E whereas those in younger (Early Jurassic) rocks strike more northerly (right histogram; adapted from Monteverde and Volkert, 2005). Extension fractures cluster into four groups based on strike and geometry including cross cutting and abutting relationships. Early (S1), intermediate (S2), and late (S3) groups of extension fractures reflect increments of tectonic stretching from the Late Triassic through the Early Jurassic. A fourth group (S3C) include mineralized cross fractures striking sub parallel to contemporary, horizontal, compressive tectonic stress directions determined from earthquake focal-plane solutions (C; Goldberg et al., 2003) and the azimuth of current tectonic plate motions (CPM; Jet Propulsion Laboratory, 2008). SC – sandstone and conglomerate facies, SS – sandstone and siltstone facies, NBF – New Brunswick fault, HF – Hopewell fault, FF – Flemington-fault, FRF – Furlong fault, CF – Chalfont fault, RF – Ramapo fault. Index map of Mesozoic basins on the East Coast (lower right) adapted from Schlische (1993).

physical relationships observed in Mesozoic rift basins throughout the eastern continental margin of North America (Sanders, 1963; Lindholm, 1978; Manspeizer and Cousminer, 1988; Swanson, 1986; de Boer and Clifford, 1988; Hutchinson and Klitgord, 1988; Lucas et al., 1988; Schlische and Olsen, 1988; Schlische, 1993, 2003). Based on these works, rifting in the Newark basin region probably began during the Middle Triassic and intensified in the latest Triassic and into the earliest Jurassic as evidenced by widespread igneous activity and a marked increase in sediment-accumulation rates (de Boer and Clifford, 1988; Schlische, 1992). Tectonic deformation and synchronous sedimentation in the region continued into the Middle Jurassic, at which time extensional faulting and associated folding may have ceased. Some time afterwards, the basin began a period of post-rift contraction, uplift and erosion (basin inversion) similar to that of other Mesozoic rift basins on the eastern North American continental margin (de Boer and Clifford, 1988; Withjack et al., 1998; Olsen et al., 1992).

3. Definition, classification, and description

Extension fractures are crack discontinuities in rock that form perpendicular to the direction of maximum incremental stretching as a result of brittle or semi-brittle failure (Ramsay, 1980; Ramsey and Huber, 1983). Extension fractures classify as joints when their two sides show no visible differential displacement (Mode I tensile fractures of Pollard and Aydin, 1988), as healed joints when the fracture walls are completely or partially joined together by secondary crystalline minerals, or as tectonic veins when a considerable thickness (>1 mm) of secondary minerals fills fracture interstices (Ramsey and Huber, 1983). In the Newark basin, steeply-dipping (>60°) to vertical extension fractures have elliptical surfaces (Fig. 2a) that are commonly straight, planar, and continuous over a distance of a few meters (Fig. 2b,d). They display characteristic surface markings including plumose patterns, rib marks and hackles that reflect their tensile origin (Pollard and Aydin, 1988). Extension fractures are considered systematic when they occur in sets within which the fractures belonging to each set are parallel or subparallel (Hodgson, 1961). In contrast, non-systematic extension fractures (Groshong, 1988) display more random orientations, often have curviplanar and irregular surfaces extending between and approximately normal to a systematic fracture set (Fig. 3). This class of extension fracture includes cross joints that commonly terminate against bedding and against other fractures (Hodgson, 1961). Cross fractures have comparatively little

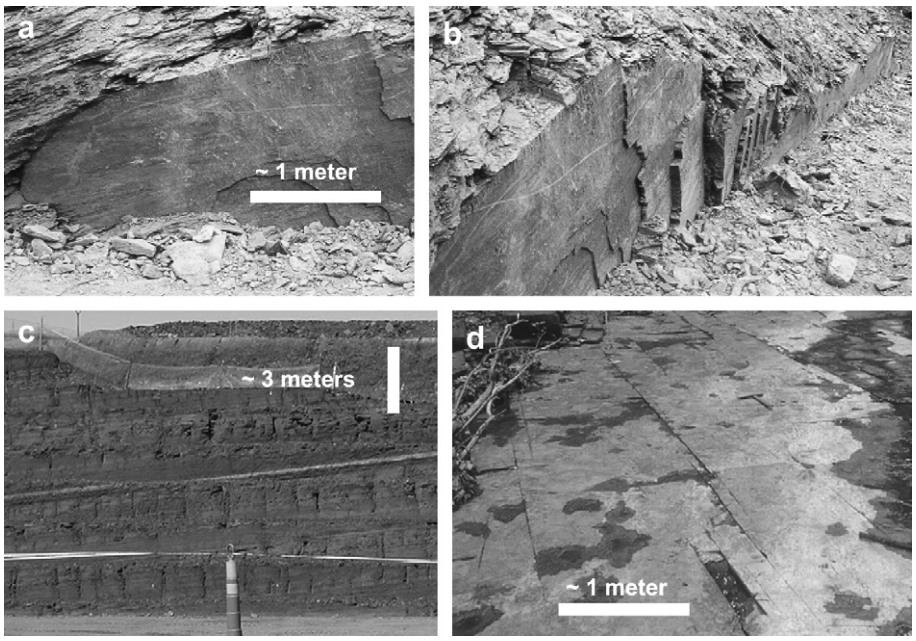

Fig. 2. Profile (a–c) and map (d) views of systematic, steeply-dipping extension fractures. These fractures are typically mapped in outcrop as joints. They dip at high angles to bedding, occur in sets with individual fractures having elliptical faces (a) and are arranged in subparallel, en échelon (stepped) alignment (b and d). They also commonly terminate against beds or abrupty change orientation and inter-fracture spacing in suprajcent sedimentary strata having having differing mechanical properties (c). Photos a and b shows joints in red mudstone of the Passaic Fm. Photo c is a benched excavation in massive-bedded red mudstone and siltstone. Photo d shows en échelon joints in the Lockatong Fm.

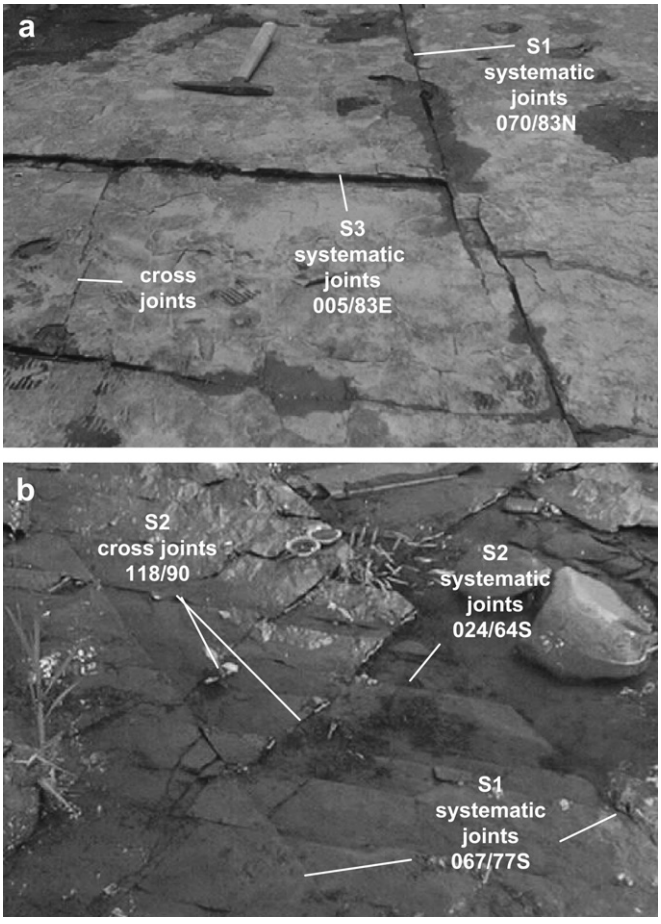

separation of fracture walls than joints and veins and have little or no associated secondary minerals filling interstices.

Steeply-dipping extension fractures in igneous and sedimentary rocks throughout the Newark Basin are mapped at, or near the land surface as ordinary joints because secondary minerals that formerly cemented space between fracture walls have been removed by mineral dissolution and erosion (Herman, 2001). In excavated and cored sedimentary bedrock sampled below the weathered zone (Fig. 4) fracture wall interstices are mostly cemented with secondary crystalline minerals (Lucas et al., 1988; Parnell and Monson, 1995; Herman, 2001). The secondary minerals include a variety of compositions and morphologies (Fig. 5) reflecting a locally variable and complex tectonic history. Vein-fill minerals include analcime, sodic feldspar (albite), potassium feldspar, calcite, gypsum, quartz, chlorite, epidote, pyrite, and relict hydrocarbons (bitumen) that generally reflect an evolved geochemical environment where early silica and carbonate cements were succeeded and locally replaced by later carbonate and sulfate cements including calcite and gypsum (Van Houten, 1964, 1965; Smoot and Olsen, 1994; Simonson and Smoot, 1994; Smoot and Simonson, 1994; Van de Kamp and Leak, 1996; El Tabakh et al., 1997, 1998). Albite (Na-feldspar) is among the early group of diagenetic cements commonly found in the Stockton Fm. and veins in the Lockatong Fm. (Fig. 6a). Calcite most commonly cements fracture walls in the Passaic Fm. with mineral fibers aligned perpendicular to the fracture plane and meeting along a central suture line (Figs. 5a,c, 6b, and 7b). These veins result from crystal growth from the vein wall inward toward the vein center as a result of repeated midpoint

Fig. 3. Different joint sets commonly interact in outcrop with late fractures both cutting across and butting into earlier sets. Non-systematic 'cross joints' are oriented about normal to, occur between, and terminate against systematic extension fractures. Cross fractures are commonly curviplanar. (a) Shows a late joint set (S3) butting into an earlier (S1) set in gray argillite of the Lockatong Fm. (b) Shows two sets of crosscutting, systematic fractures and S2 cross joints in gray argillite of the Lockatong Fm. Brunton compass shown for scale in upper center view of bottom photo.

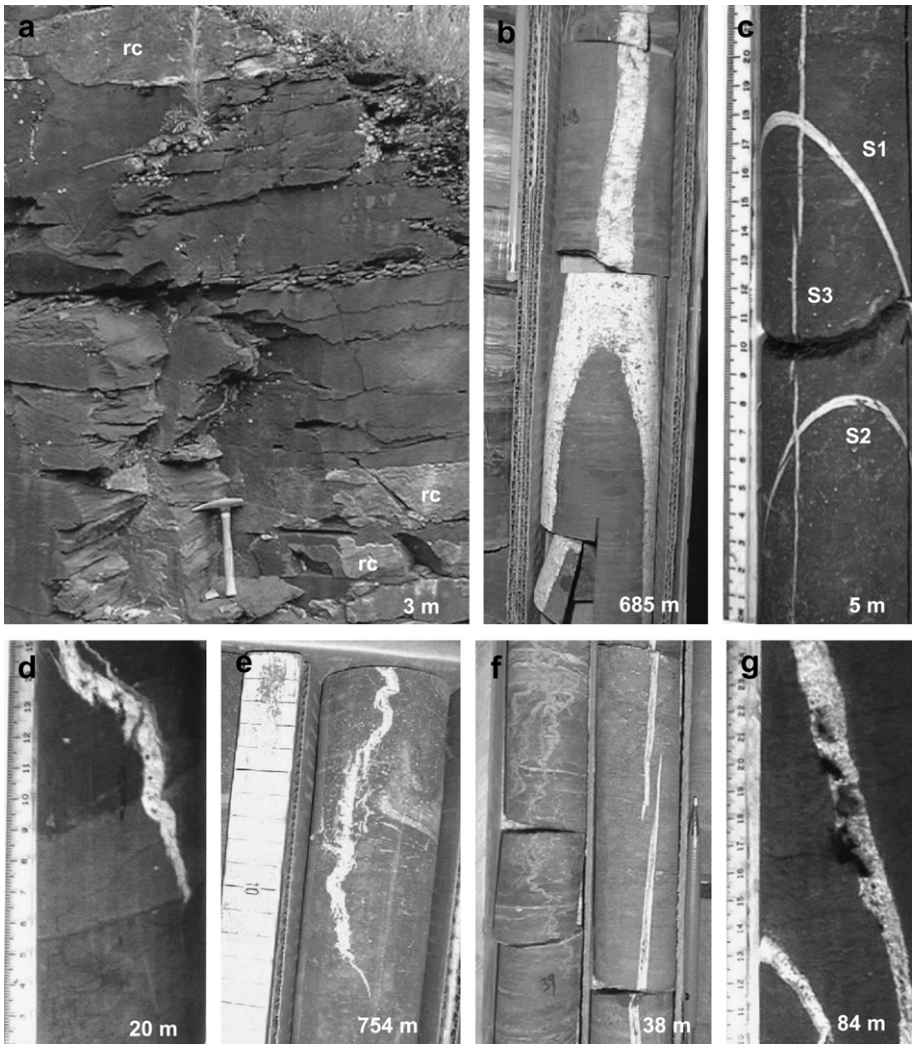

Fig. 4. Extension fractures in the subsurface are mostly filled with secondary crystalline minerals such as calcite and classify as tectonic veins. Systematic joints mapped at the surface were also probably veins, but now appear as joints because secondary minerals were dissolved (a and g) through interaction with weakly acidic ground water. (a) Shows remnant calcite (rc) on fracture walls along a railroad excavation. (b and f) Show veins in the middle part of the Passaic Fm. from the Rutgers deep core (Olsen et al., 1996a). (c, d and g) Show veins in the middle Passaic Fm. from a 2-inch -diameter core. (e) Show veins and folded, clay-filled mudcracks in the lower part of the Passaic Fm. from a 2-inch -diameter core. Depth below land surface is indicated in the lower right part of each figure.

fracturing accompanying progressive dilation and crack-seal episodes (Durney and Ramsay, 1973; Groshong, 1988). Many of these veins have early albite grown on the fracture walls that are overgrown by calcite (Fig. 5a). Some fibrous calcite-filled veins display twinned calcite (Fig. 5a) from mechanical strain associated with either localized tectonic compression (Lomando and Engelder, 1984) or deep burial (El Tabakh and Schreiber, 1998). Other cements have curved and sheared fibers (Fig. 5c, and Lucas et al., 1988), indicating local rotations of the incremental stretching direction and late shearing. Complex vein-fill cements have composite vein morphologies with relict grains of albite and K-spar embedded in a matrix of mosaic calcite with intergrown pyrite and bitumen (Fig. 5b). Also common are veins of one strike set branching or splaying into a new strike orientation representative of later extensional phases (Fig. 6a). Early veins are locally crosscut and overprinted by later vein sets having a different strike orientation (Figs. 4c and 6b).

Gypsum-filled veins (Fig. 6c) represent a unique class of fracture for they cut across all earlier structures and are oriented sub-horizontal and therefore orthogonal to the aforementioned tectonic extension veins. These gypsum veins variably lack central sutures, have morphologies linked to episodic growth and linkage, but are late-stage veins that may have resulted from unloading and exhumation (El Tabakh et al., 1998) or perhaps, from late tectonic compression.

4. Distribution, geometry, and finite strain

Steeply-dipping extension fractures mapped in a 750-sq. km. area in the central part of the basin group into four strike maxima (Fig. 1). Three of these groups (S1–S3) have pronounced maxima striking subparallel to map traces of large normal faults. The S1 group includes fractures striking NE–SW (N36° – 70° E) subparallel to the basin's northwestern, faulted margin. A second (S2) group strikes NNE–SSW (N11° – N35° E) subparallel to the main segments of intrabasin faults in New Jersey and most Early Jurassic dikes in Pennsylvania (Fig. 1). A third group (S3) strikes N–S (N10°E–N20°W) subparallel to normal faults in Early Jurassic rocks cropping out in the eastern part of the basin (Monteverde and Volkert, 2005; Volkert, 2006a,b). S1 and S2 groups have pronounced strike maxima

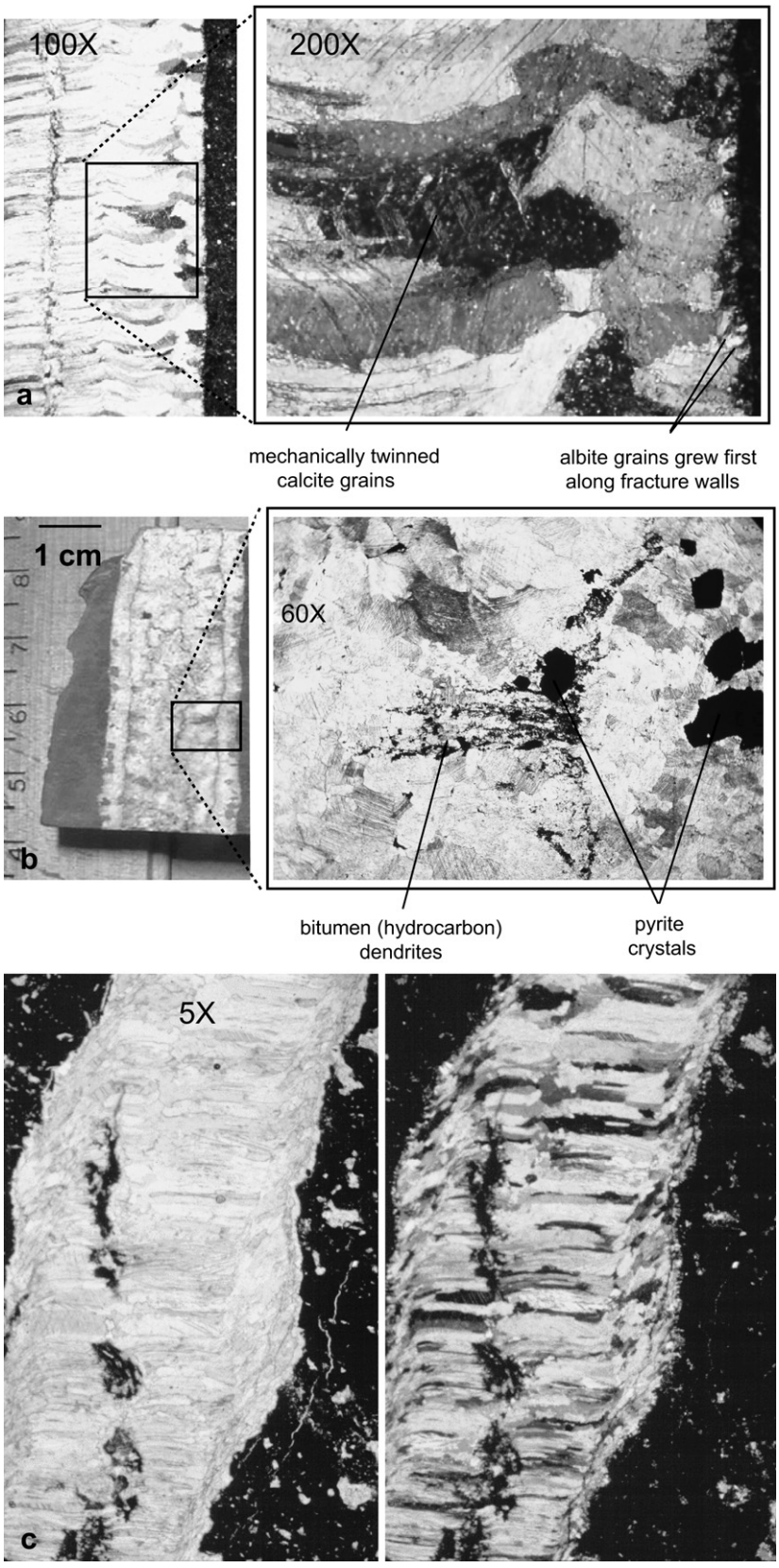

Fig. 5. Examples of vein-fill minerals and morphologies. Calcite fibers are locally curved and mechanically twinned and postdate early albite growths along the fracture walls (a). Sample from gray mudstone in the lower part of the Passaic Fm. Some veins (b) are filled with mosaic calcite crystals containing interspersed sulphides (pyrite) and hydrocarbons. Sample of gray mudstone, Rutgers deep core (Olsen et al., 1996a) at 685 m depth. Other veins (c) have straight calcite fibers oriented at high angles to fracture wall and localized shearing along the walls and vein sutures. (c) Shows vein cutting red mudstone under plane (left) and polarized (right) light.

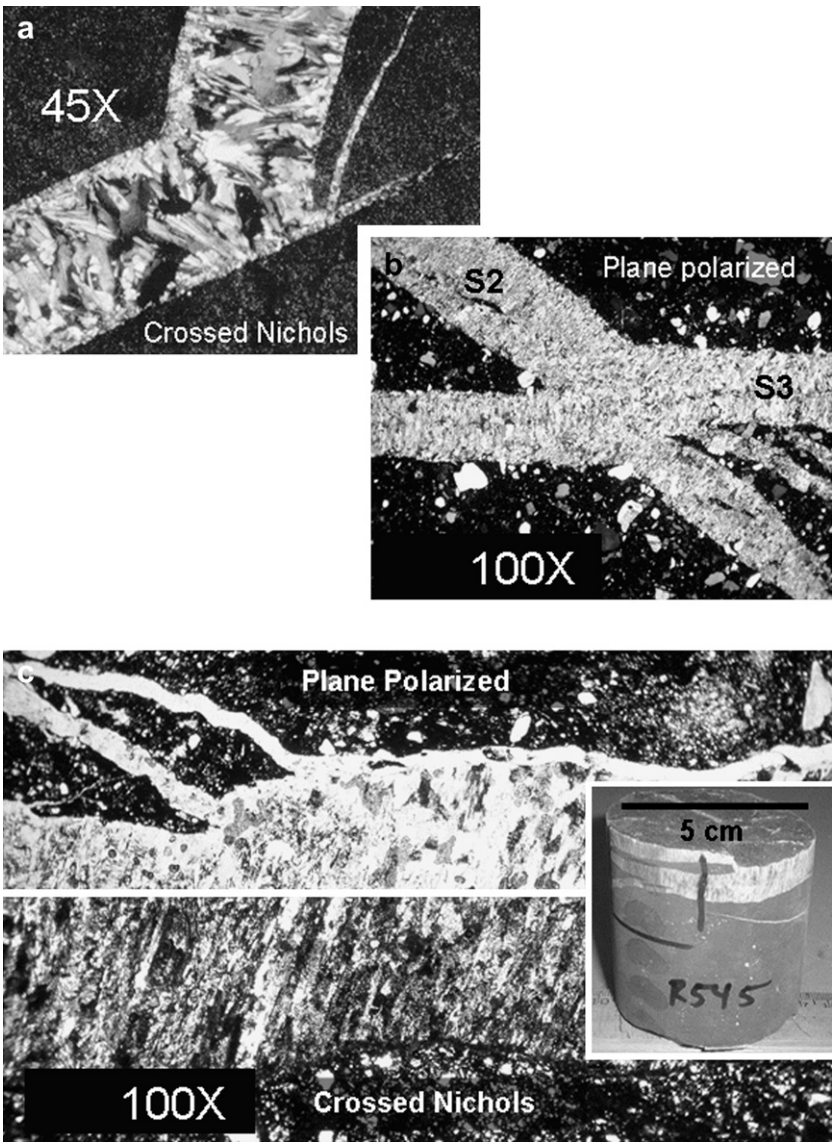

Fig. 6. Common vein-cementing, secondary minerals inlcuding albite and calcite. (a) Albite-filled veins in gray argillite of the Lockatong Fm. (b) Fibrous calcite veins in red mudstone of the Passaic Fm. Calcite fibers of a later vein set cut across and overprint calcite fibers in an earlier set. Vein mineralogy locally reflects host rock geochemisty. The Na- and Si-rich Locaktong Fm. commonly has albite cements (a) and the carbonate and sulfate-rich Passaic Fm. commonly has calcite- and gypsum-cemented veins (b). Gypsum veins (c) are late veins, mostly oriented subhorizontal with subvertical crystal fibers. Gypsum veins many cms thick are found at depths exceeding 60 m in some NE and central parts of the basin. Photomicrograph of calcite veins in b show a S3 vein cutting an older S2 vein (core sample in Fig. 4c).

of N36° – 50°E and N16° – 30°E respectively, in the center of the basin (Fig. 1). S1 through S3 fracture groups coexist with sets of coeval cross fractures so that many different fracture sets can mark a single location (Fig. 3). More commonly, only one or two steeply-dipping fracture sets are seen in any single outcrop (Fig. 2). The fourth (S3C) group of steeply-dipping extension fractures strike within a 40° sector ranging about E–W (Fig. 1). The SC3 group parallels S2 and S3 cross fractures, align with directions of contemporary, regional compressive stresses (Goldberg et al., 2003) and are more limited in their spatial distribution. Other gently to moderately dipping fractures sets scattered throughout the basin include mineralized shear fractures, cooling fractures in igneous dikes, sills, and basalt flows (Faust, 1978), and non-systematic fractures near the land surface developed from weathering, erosion, and unloading. The gently to moderately dipping shear fractures locally cut diabase intrusions and warped strata in faulted hanging walls. These fractures may partly stem from regional, late-stage tectonic compressions. Nevertheless, the S1 through S3 extension fractures are by far the most prevalent tectonic fracture sets in the basin and is the focus here.

S1 through S3 extension fractures show some similar geometric and spatial properties. For example, the surface area of extension-fracture walls, and the spacing between fractures measured normal to a fracture surface commonly decrease with the thickness of the fractured layer; a feature observed in sedimentary rocks elsewhere (Pollard and Aydin, 1988; Huang and Angelier, 1989; Narr and Suppe, 1991; Gross, 1993). Inter-fracture spacing, or fracture density, is measured normal to fracture walls and locally ranges from less than 1 fracture per meter to more than 50 fractures per meter near the trace of mapped faults (Herman, 1997). Fracture trace lengths of <1– 5 m are common in all bedrock units, and mechanical (fracture) layering in sedimentary strata commonly ranges from < 1 m to about 2 m thick (Fig. 2c). Most of these fractures are aligned en échelon with adjacent and overlapping,

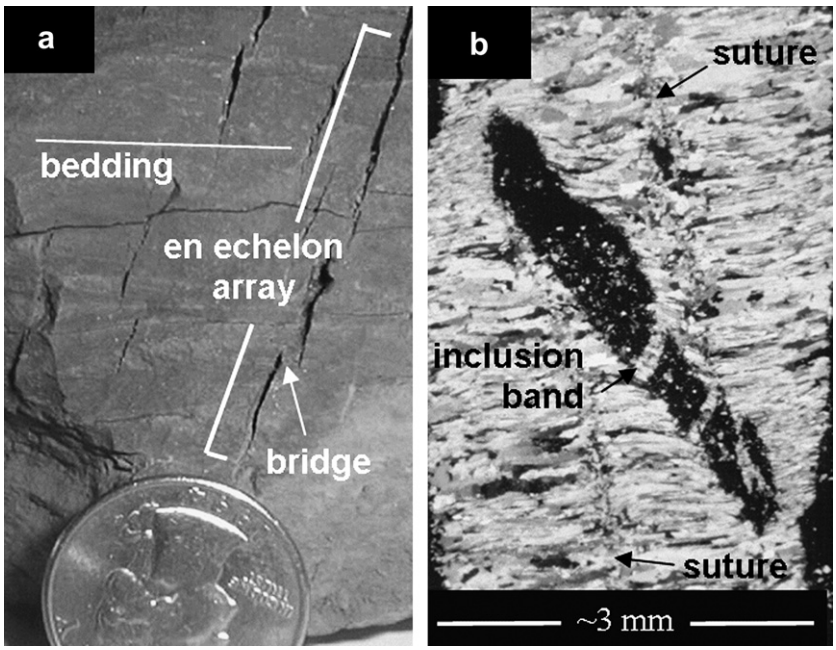

Fig. 7. Steeply-dipping extension fractures in the Passaic Fm. are commonly filled with fibrous calcite with centralized sutures indicating synchronous filling or healing of the fracture during opening and growth. Fractures grow by linking smaller fractures into larger ones. (a) Shows a hand sample of veins in red mudstone from the Passaic Fm. Photomicrograph b shows 'syntaxial' vein morphology (Durney and Ramsay, 1973) with calcite-mineral fibers in optical continuity with calcite grains along the fracture walls. Fibers grew from the fracture walls toward a central suture line located about midway between the walls. Included bands of red mudstone in the central field of view (b) show that fractures coalesce through growth and linkage and capture bridges (a) otherwise separating adjacent, en échelon fractures.

subparallel veins displaying systematic, stepped geometry (Figs. 2b,d, 3a, 4c,g, 7a, 8 and 9). Curved country-rock bridges are commonly positioned between adjacent, isolated veins (Figs. 7 and 9a) or occur as remnant country-rock inclusions encased by secondary mineral cements from linkage and growth of fractures (Fig. 7b). Steeply-dipping sets of en échelon veins are locally arranged in conjugate arrays (Fig. 9) having the geometry of normal dip-slip shear zones (Type 2 arrays of Beach, 1975). As such, these fractures qualify as transitional-tensile fractures (Van der Pluijm and Marshak, 1997; Engelder, 1997) because individual cracks occur as Mode I (pure opening) features but act in concert to impart shear strains in layered strata. They form in a tectonic environment having principal sub-horizontal tension and sub-vertical principal compression (Fig. 9b). Their formation and growth as en échelon structures is a mechanism by which strata are stretched in both horizontal and vertical directions while imparting gentle stratigraphic dips in a direction normal and opposite to that of dipping fracture surfaces (Figs. 10–12). Stratigraphic dips resulting from transitional-tensile fracturing represents only a small percentage of current dip values (Fig. 12) that reflect many, cumulative strain processes including rotational slip on major faults and regional tilting accompanying basin inversion. Nevertheless, spaced sets of tectonic veins developed in the basin as a pervasive strain mechanism allowing a thick pile of heterogeneous layered rocks to simultaneously stretch and sag (Fig. 13). Tightly spaced swarms of veins probably served as loci for subsequent fault development in agreement with the reported dynamics of Type 2 en échelon cracks where crack arrays weakened a rock mass and later served to localize shear zones (Nicholson and Pollard, 1985).

Sedimentary bedding in Late Triassic rocks, igneous layering in Early Jurassic diabase and basalt and associated fractures are also being mapped using digital borehole televiewers (BTV) including both optical (OPTV) and acoustical varieties. Since 2001, the NJGS has acquired and analyzed stratigraphic layering and fracture orientations from more than 30 locations in the basin including over 120 wells (Herman, 2006a). BTV records are of 6- and 8-inch-diameter water wells ranging in depths to about 180 m below land surface. Processed BTV records (Fig. 14) provide information on the distribution and arrangement of fractures in the shallow subsurface that become an integral part of hydrogeological framework interpretations developed for ground-water-resources projects

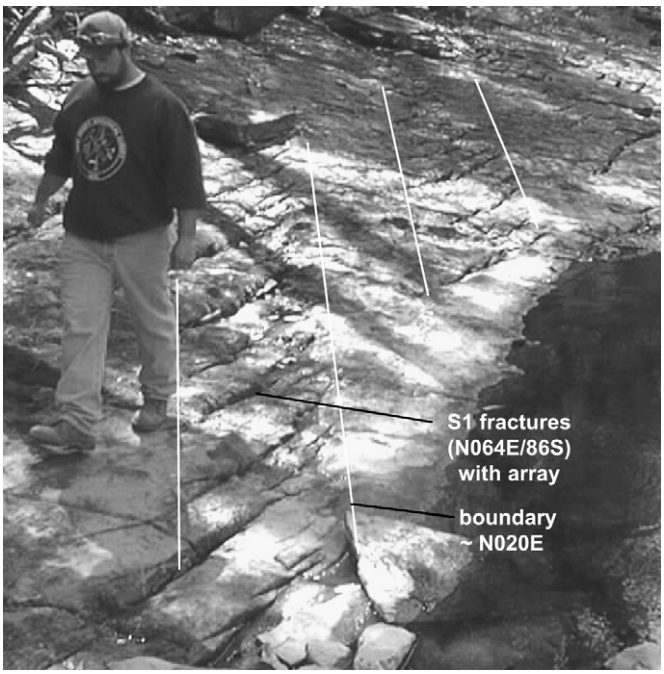

Fig. 8. S1 (early) fractures arranged en échelon in spaced arrays with boundaries having S2 orientations. S1 fractures have tips that locally curve into alignment with later extension and cross fracture strikes. Outcrop of Lockatong Fm. red argillite.

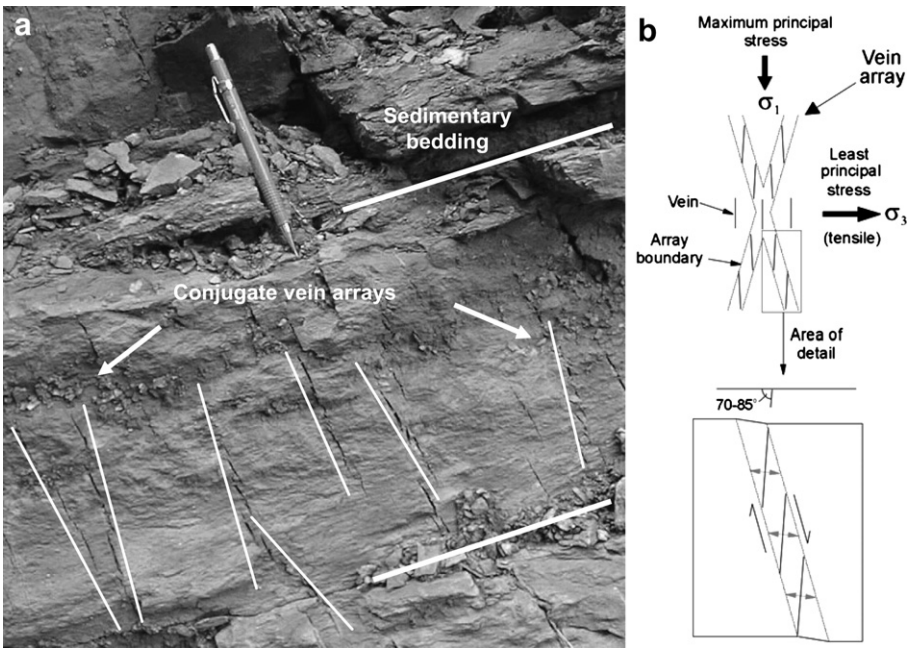

Fig. 9. Steeply-dipping, en échelon extension fractures locally form conjugate arrays (a) having the geometry of normal dip-slip shear zones (b). (a) Shows profile view of vein arrays in Passaic Fm. red mudstone in the hanging wall of the Flemington fault. These S2 veins average about 70° dip when bedding is restored to a pre-tilt (horizontal) alignment (Fig. 11 and Herman, 2001). This value directly agrees with the angle of inclined-shear failure reported for material moving in faulted, extended hanging walls (Xiao and Suppe, 1992; Dula, 1991; Withjack et al., 1995).

(Herman, 2001, 2006a,b). OPTV records are used here to further demonstrate S1 through S3 fracture distributions and geometry, including fracture-group interactions. OPTV records commonly provide detailed, visual records of small-scale structural relationships, including localized, normal dip-slip shear offset of sedimentary strata across small faults having the same orientation as associated extension fractures (Figs. 15b and 16a,b).

Relative ages of the different fracture groups is based on fracture morphology and interactions as seen in the outcrop and BTV data, and the spatial distribution of the different groups in the stratigraphic sequence; S1 fractures are older than S2, which are older than S3. S1 veins occur with the highest frequency in the older, Late Triassic sedimentary rocks including the Stockton, Lockatong and the lower parts of the Passaic Fm., where they are locally folded

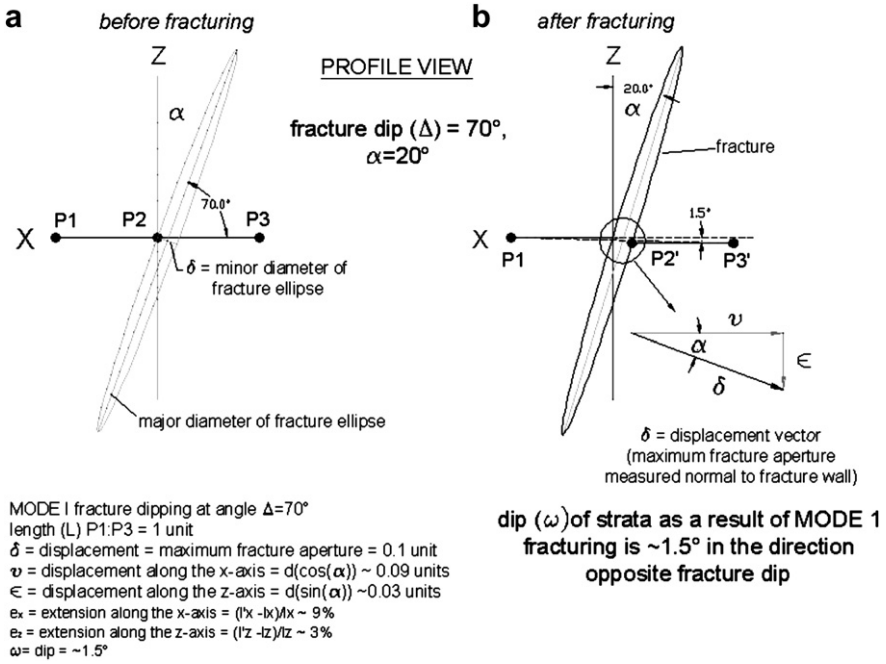

Fig. 10. Finite strain analysis of a steeply-dipping, Mode I crack in profile. (a) The trace of the pre-fractured, horizontal, strata surface corresponds with the *x*-axis. After fracturing (b), strata are positively extended in the stretching direction (e_x) and apparently rotated in a direction opposite that of fracture dip ($\Delta = 70^\circ$) as a result of fracture opening. Displacement of reference points P2 and P3 along the *x*-axis into their fractured positions (P2′ and P3′ in b) illustrates how steeply-dipping fractures impart stratigraphic dip across fracture interstices. This exercise shows that a fracture dipping at 70° with a fracture aperture to inter-fracture spacing ratio of ~ 1/10 imparts ~9% horizontal stretching, ~3% vertical stretching, and ~1.5° apparent stratigraphic dip in the direction opposing fracture dip.

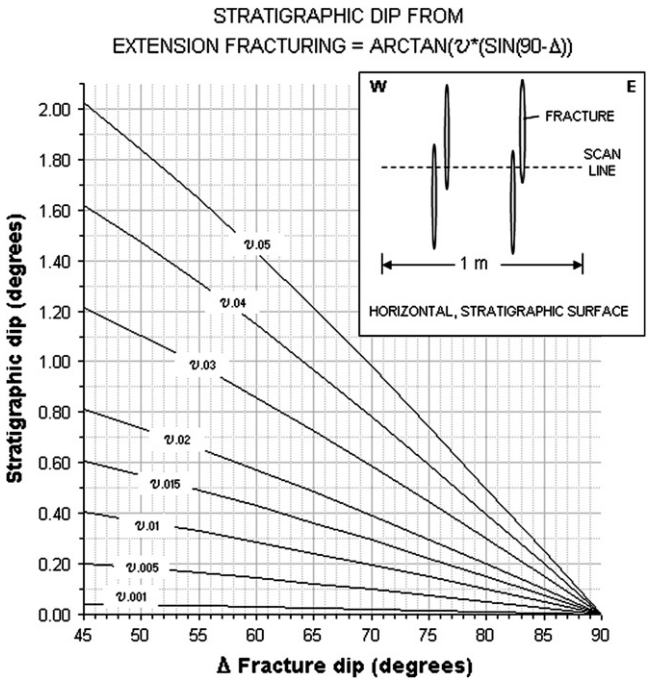

Fig. 11. Graph of an analytical solution for determining the component of stratigraphic dip resulting from Mode I fracturing. The solution provides a measure of stratigraphic dip as function of fracture dip (Δ) and total apparent fracture aperture (υ-meters). The solution is derived using the strata-fracture geometry outlined in Fig. 10 and is designed for use with field measurements of Δ and υ per meter distance measured along a horizontal scan line. υ is an apparent value because apertures are measured along a stratigraphic surface, but true fracture apertures occur normal to fracture dip as shown in Fig. 10. An average Δ is used after restoring fractures to pre-strata-tilt orientation as illustrated in Fig. 12. υ is measured along a scan line oriented parallel to fracture-dip azimuth in either a map or profile plane. An example of this application is illustrated in the upper right diagram. In this case, a 1-m scan line crosses four fractures cutting a horizontal stratigraphic surface. Assuming $\upsilon = 2$ cm (0.02 m) and fracture dip (Δ) = 70°E, then the dip angle resulting from fracturing = ARCTAN (0.02 * (SIN (90–70))) = 0.39°W.

normal to bedding (Figs. 4e,f and 15a) from sedimentary compaction during burial and lithification. In contrast, compaction folding of S2 veins is rare and folding of S3 veins has not been observed. Moreover, S1 veins have the most complex vein-fill morphologies including crack-seal banding and recrsytallization of vein-fill with mosaic calcite (Figs. 4b and 5b) and localized hydrothermal alteration (bleaching) of fracture walls from the reduction or removal of iron as hematite. Hydrothermal fluids convectively circulating in basin strata during the Late Triassic to Early Jurassic caused localized high-temperature (>100 °C) alteration of earlier diagenetic minerals (Steckler et al., 1993; Van de Kamp and Leake, 1996).

S2 fractures occur with higher frequency in the upper part of the Passaic Fm. and Early Jurassic strata (Figs. 1 and 18). They commonly have simple, straight mineral fibers filling fracture interstices (Figs. 6b and 7b) and are seen crosscutting and terminating against (butting into) S1 fractures (Figs. 3b and 17b). The structural link between S1 and S2 fractures is locally seen in outcrop where fringe cracks (Younes and Engelder, 1999) with hackly surfaces bridge S1 and S2 fractures (Herman, 2005a). These cracks propagate away from S1 fracture tips and curve towards and into S2 fractures, thereby preserving evidence of the geometric transition between the overlapping fracture sets and their relative ages. In places, S1 veins form en échelon arrays with crack tips and hackles that gradually twist into alignment with array boundaries having later S2 strikes (Fig. 8). S1 fractures also open along S2 azimuths in outcrop where these two fracture systems overlap (Herman, 2001a).

S3 fractures are late-stage extension fractures that cut across, and locally terminate against both S1 and S2 earlier sets (Figs. 3a, 4c, and 17c). S3 fractures occur with the highest frequency in the northeast parts of the basin where Early Jurassic strata crop out, especially along N–S striking fault segments near mapped fault tips of intrabasinal fault systems (Figs. 1 and 18). S3 and S3C extension fractures also occur in southeast parts of the basin north of the Trenton Prong where E–W striking, late-stage, wrench faults are mapped (Herman, 2005a).

5. Fracturing with respect to the age of strata, faulting and tectonic plate motions

Steeply-dipping extension fractures are an integral part of the basin's structure. They record accumulated brittle strain as part of the regional tectonic history. Their orientation, distribution, morphology and vein-fill mineralogy record incremental strains and variations in pore-fluid chemistries developed throughout the tectonic history of the basin beginning in the Late Triassic. There are no radiometric age dates reported for fracture-fill minerals in the Newark basin, but the ages of the different fracture groups are constrained by the rocks they affect.

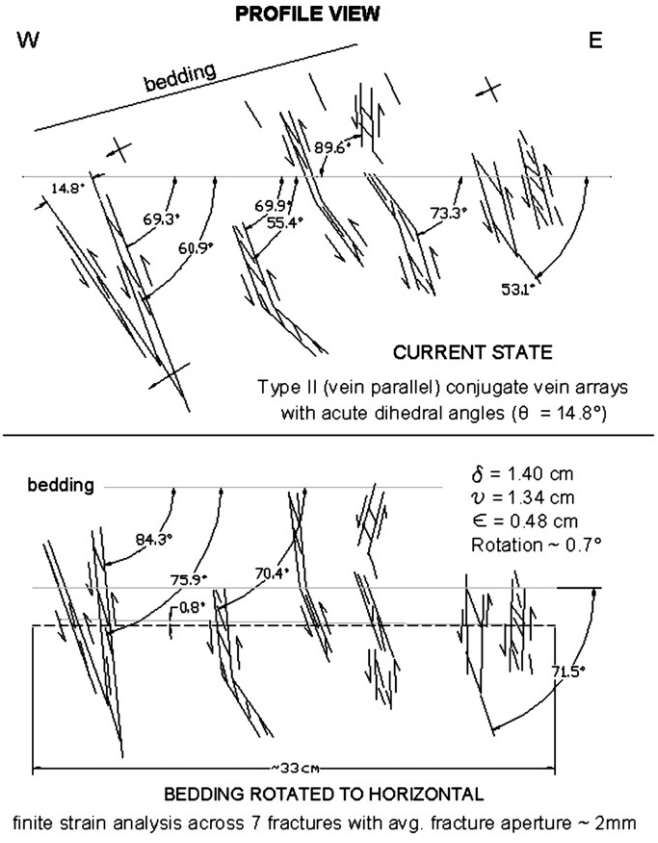

Fig. 12. Finite-strain analyses (profile view) of the vein arrays shown in Fig. 9a. In the current state (a) fractures dip about 55–65° within array boundaries dipping 70–90°. Array-boundary dihedral angles range from ~15 to 30°. Fracture dip (Δ) averages ~73° E after rotating bedding 15° clockwise to horizontal (b). For the strain analysis (b), a reference (dashed) line 33 cm long was drawn parallel to horizontal bedding across seven steep fractures having an average fracture aperture of ~2 mm for a total fracture aperture of ~0.014 mm. Based on the solution specified in Fig. 11, the observed fracture properties are extrapolated to a 1-m interval. Therefore, υ = (3 * 0.014 m) ~ 0.04 m and bed rotation attributed to Mode I fracturing is: ARCTAN (0.04 * (SIN (90 −73))) ~ 0.7°W. Thereforein this case, steeply-dipping extension fractures stretched bedding ~ 4% (1.32 cm)/ (33 −1.32 cm)) and accounts for ~ 5% (0.7° / 15°) of current bedding dip.

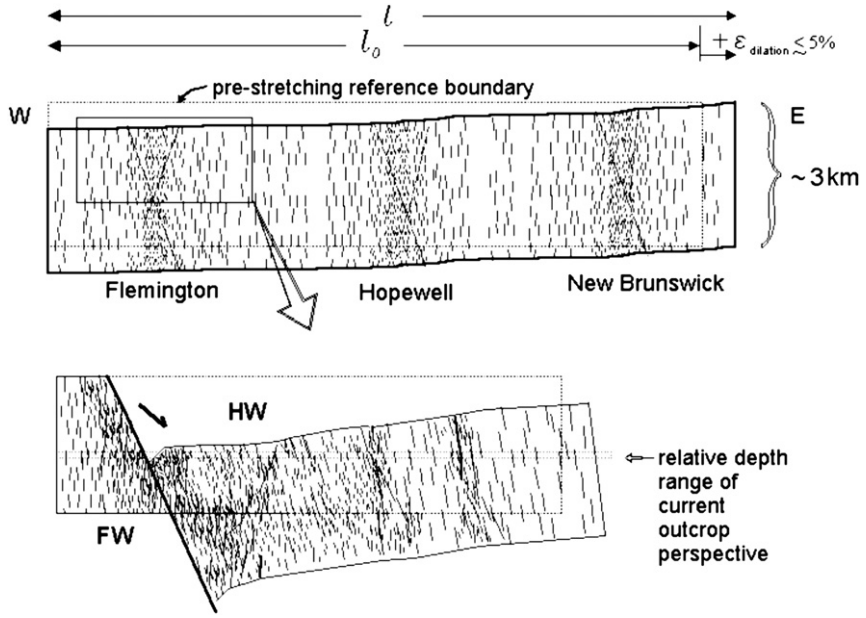

Fig. 13. A schematic profile of basin strata showing progressive strain associated with the development of punctuated S2 fracture sets from Flemington to New Brunswick, NJ. Map trace of profile shown on Fig. 18.

S1 fracture sets occur most frequently in Late Triassic rocks (Fig. 1). Compaction-folded S1 veins (Figs. 4e,f and 15a) occur in strata within hanging wall blocks of the border faults and subparallel segments of the Hopewell fault system. They reflect early extension and lithologic compaction accompanying sedimentary loading. These relations, together with having S1 fractures and brittle deformation zones occurring locally in Early Jurassic diabase (Herman, 2005a) indicate a prolonged phase of S1 tension directed normal to the structural axis of the basin through the Late Triassic and into the earliest Jurassic period (Fig. 19).

The structural transition between S1- and S2-phase fracturing appears to have been continuous based on the aforementioned occurrence of gradual twist hackles bridging S1 and S2 fracture surfaces. However, these bridging structures are physically small in comparison to much larger and well organized S1 and S2 surfaces and therefore may signal a relatively abrupt reorientation of an evolving, regional stress field. S2 maxima are aligned about 20–30° counterclockwise with respect to S1 maxima (Fig. 1). This reflects clockwise, incremental rotation of the stretching direction for the developing continental margin (Fig. 19) preceding the onset of seafloor spreading sometime during the Early to Mid Jurassic (Benson, 2002). Overlapping fractures and faults having acute angular arrangements agree with overlapping and stepped fault arrangements in analog clay model and sandbox studies of oblique-rift and strike-slip models (Schlische et al., 2002; McClay and Bonora, 2001).

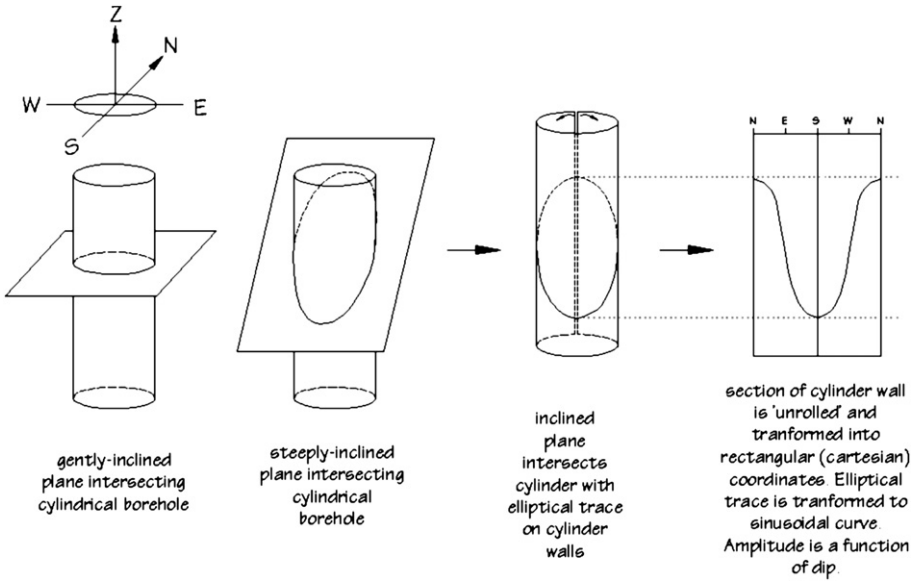

Fig. 14. Schematic diagram illustrating how cylindrical BTV records are processed by 'unwrapping', flattening, and transforming borehole data. The trough of the trace (or the bottom of the 'V') gives the structure dip azimuth. Higher dips correlate with sharper Vs.

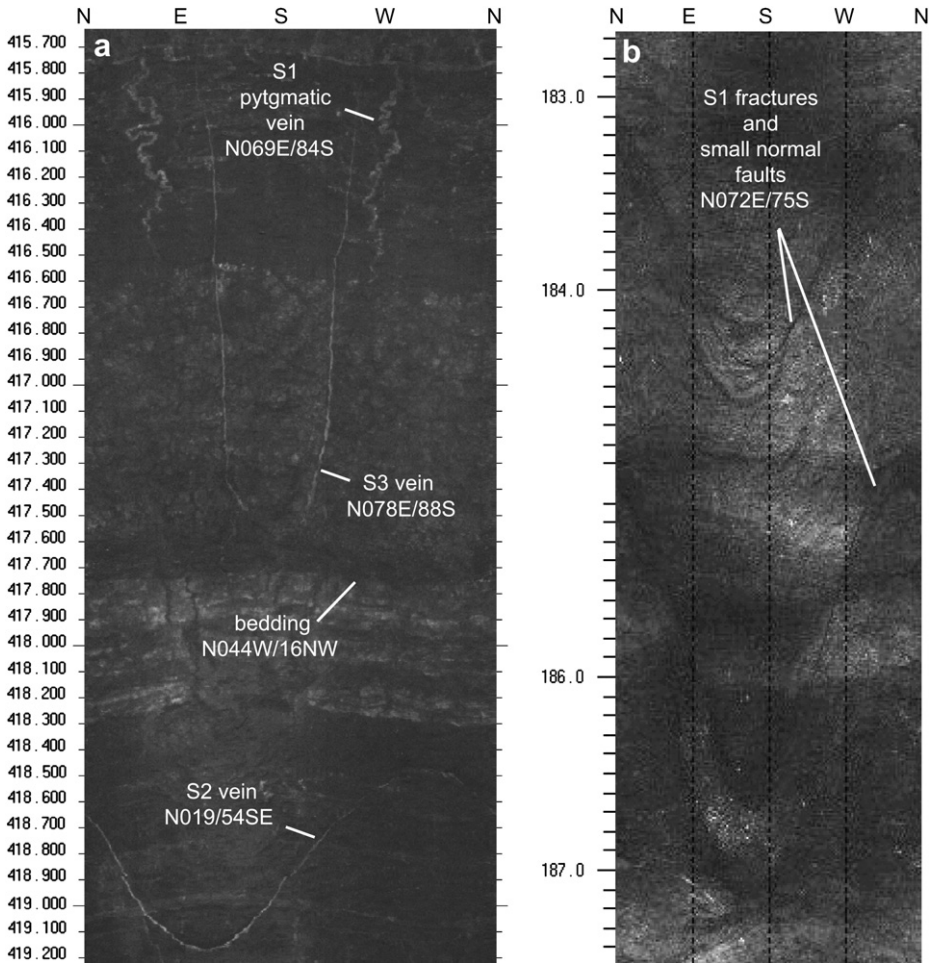

Fig. 15. OPTV records of red and gray argillite in the Lockatong Fm. showing bedding and fracture geometry. (a) Shows early, pytgmatic-folded S1 vein, other S2 and S3 veins and bedding. (b) Shows S1 extension and shear fractures with normal dip-slip shear offset of beds. Record processsing annd dip azimuth/dip values determined using Robertson Geologging Ltd. RGLDIP vers. 6.1 (2000) software. Depths below land surface (bls) indicated in feet.

S2 fractures sets in the Passaic Fm. are mostly cemented with fibrous calcite, are rarely folded by lithologic compaction, and therefore postdate lithification of most Late Triassic sedimentary deposits. S2 fractures occur with the highest frequency in uppermost parts of the Late Triassic Passaic Fm., in Early Jurassic rocks (Figs. 1 and 18), and near mapped traces of major, intrabasinal fault segments of the Flemington (Herman, 1997), Hopewell (Monteverde et al., 2003) and New Brunswick fault systems (Stanford et al., 1998). These crustal-scale faults locally splay from and strike obliquely to the northwestern border faults (Fig. 1) and probably developed from the coalescence of S2 tension fractures distributed in punctuated swarms throughout the center of the basin (Fig. 13). The S2 extension phase reflects a period of accelerated crustal stretching and basin subsidence that affected continental crust throughout the region beginning sometime during the Early Jurassic. Late Triassic bedrock and older basement are also intruded by Early Jurassic igneous dikes having S2-maximum alignment in the southwest part of the basin (Fig. 1). Laney et al. (1995) mapped late-stage leucocratic dikes, zoned veins, hydrothermal veins, and strike-slip faults of S2 alignment cutting the Lambertville diabase sill. Merguerian and Sanders (1994) mapped chevron folds plunging N75°W in the Lockatong Fm. at the base of the Palisades sill in northern New Jersey. They interpreted these folds as resulting from intrusive flow emplacement toward the NE, normal to the S2 stretching direction outlined here. The body of evidence therefore points to S2 extension fracturing lasting throughout the estimated ~ 580 Ky duration of magmatic activity in the basin (Olsen et al., 1996b) beginning near the close of the Late Triassic at about 201 Mya (Sutter, 1988; Dunning and Hodych, 1990). S2 extension on existing faults of S1 strike would have resulted in oblique-normal slip reactivation on the border faults as reported by Ratcliffe and Burton (1985).

The structural transition between S2- and S3-phase fracturing is also apparently continuous, resulting in upward-twisting fractures and faults reflecting another ~30° counterclockwise reorientation of the principal stretching direction postdating lithification of Early Jurassic basalt. Steeply-dipping faults in the New Brunswick fault system having S2 strikes curve into S3 alignment near fault tips cutting Early Jurassic basalt of the Watchung Mt. region (Fig. 18). Upward twisting, curvilinear jointing in these basalts reported by Faust (1978) also record this incremental, rotational strain.

S3 fractures are more locally restricted in their occurrence than both S1 and S2 groups and more problematic with respect to their tectonic history, insofar as they appear to stem both from a late phase of continental extension, then subsequent compression. During late-stage, S3 extension, the basin was stretched E–W to ENE (in its current orientation) with concurrent development of N–S to WNW striking, high-angle, oblique-slip normal faults. These faults splay into late-stage, E–W striking oblique faults including the Chalfont fault in Pennsylvania (Herman, 2005a,b). Late-stage,

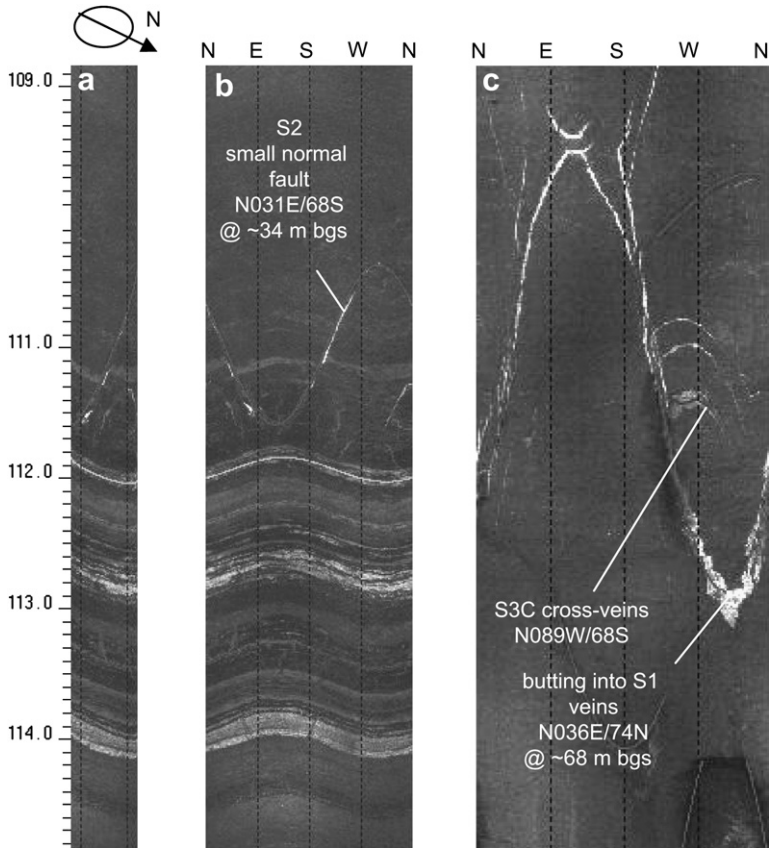

Fig. 16. OPTV records including a virtual, wrapped core (a) and unwrapped display (b) showing a S2 small normal fault and veins, and S3C veins butting into S1 vein (c). Records on left are in Passaic Fm. red and gray mudstone and black shale. c is of Passaic Fm. red mudstone. Depths below land surface (blls) indicated in feet in a.

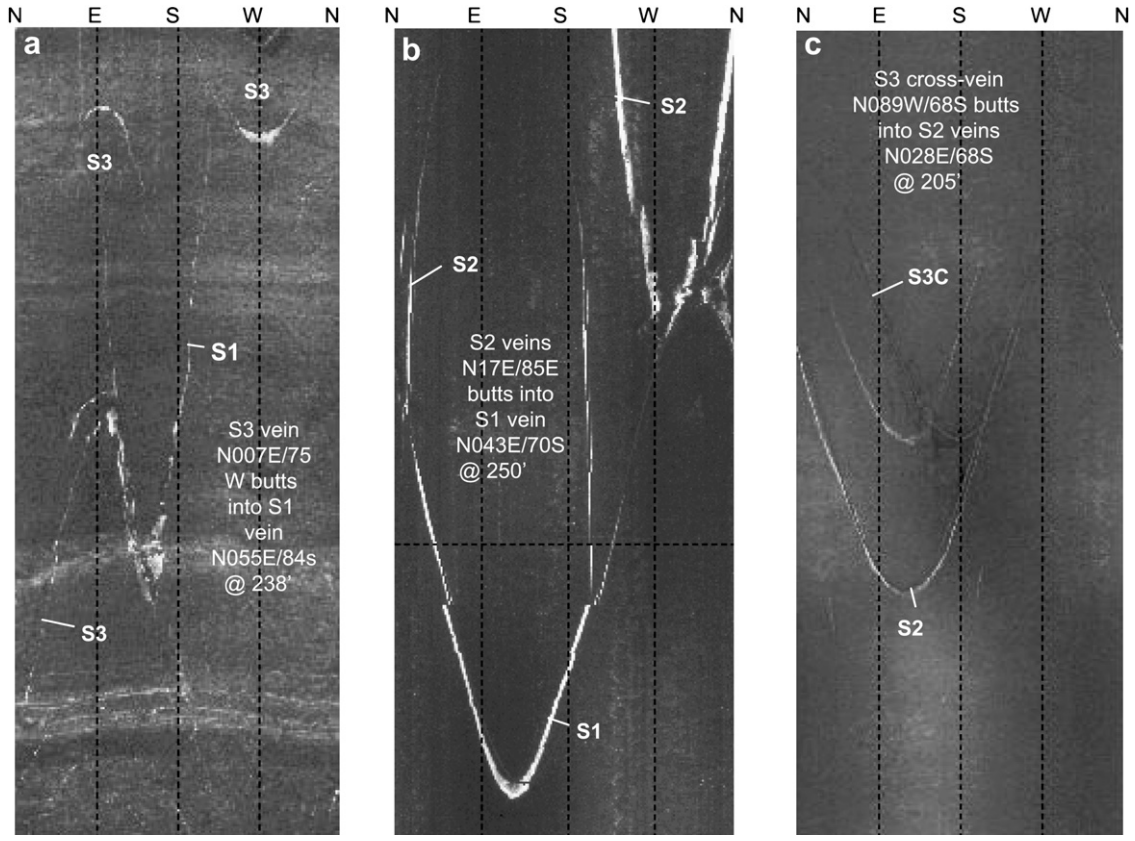

Fig. 17. Fracture geometry from three OPTV records. (a) Shows S3 vein butting into S1 vein in red and gray argillite of the Lockatong Fm. (b) Shows S2 veins butting into S1 vein in the lower part of the Passaic Fm. (c) Shows S3C vein butting into S2 vein in red mudstone from the middle part of the Passaic Fm.

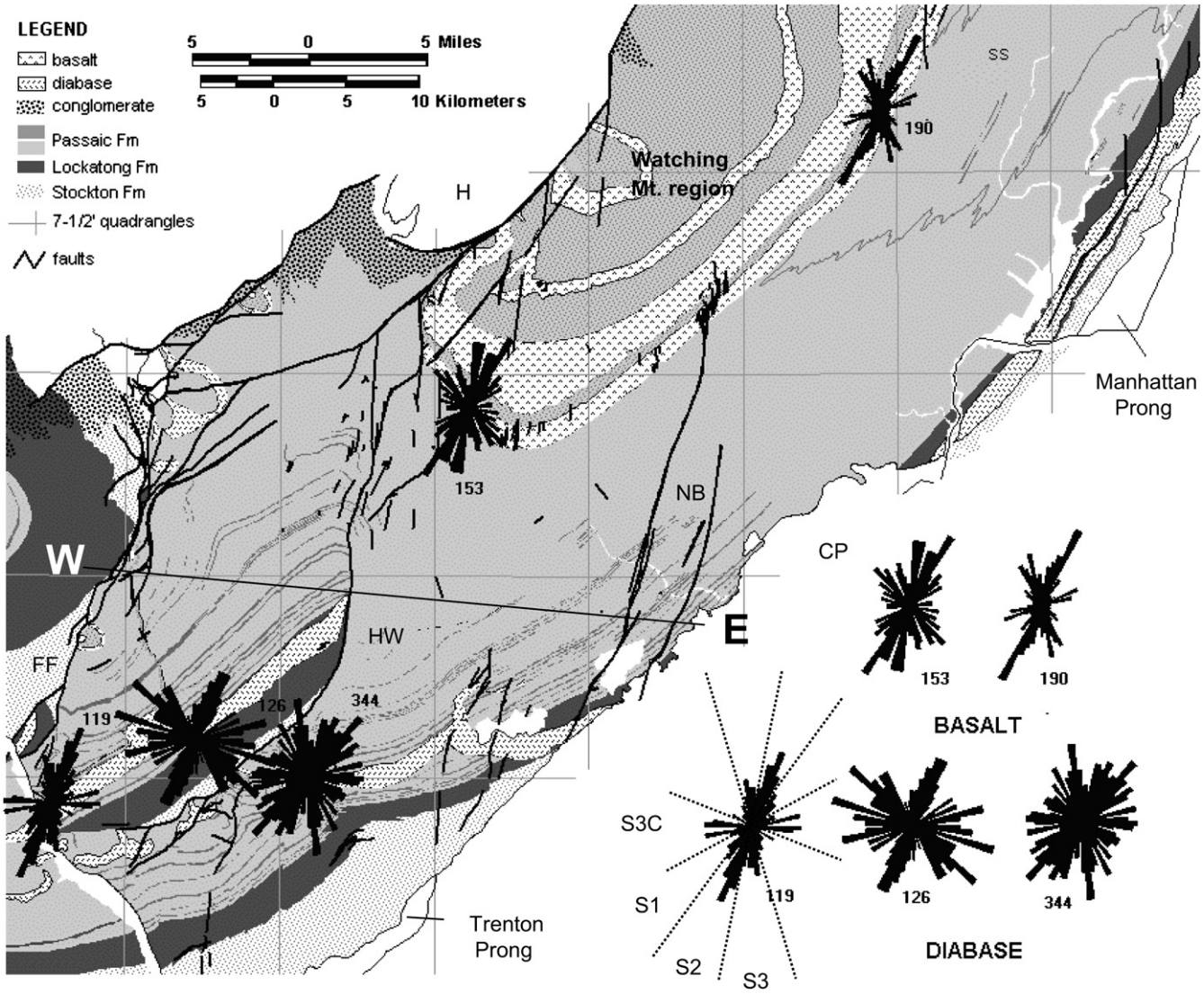

Fig. 18. Bedrock geology of the east-central part of the basin showing circular histogram summaries of OPTV fracture data from five locations in Early Jurassic basalt and diabase. Numbers beside the histograms indicate fracture sets measured at each site. West to east profile trace corresponds to schematic profile interpretation in Fig. 13. SS – sandstone and siltstone facies of the Passaic Fm., NB – New Brunswick fault system, HW – Hopewell fault system, FF – Flemington Fault system, H – Highlands province, CP – Coastal Plain.

leucocratic, igneous dikes as much as a couple of meters thick and smaller, zoned veins also cut Early Jurassic diabase sills at steep angles along S3 trends near the Hopewell fault (Laney et al., 1995; NJ Geological Survey library notes on the Pennington Diabase quarry). These S3 extension fractures, dikes, and faults cut across and offset S1 and S2 features and therefore indicate a finite, counterclockwise rotation of the principal extension direction in the region of about 50–60° before the onset of the regional tectonic compression and basin inversion (Fig. 19).

Mineralized S3C cross fractures have also been mapped in Early Jurassic basalt and diabase and in Late Triassic sedimentary bedrock north of the Trenton Prong in the hanging wall of the Hopewell fault (Herman, 2005a). They strike about E–W, are complimentary in strike to S3 extension fractures, and may represent late-stage dilation and mineralization of earlier, curviplanar, non-systematic cross fractures optimally aligned for reactivation and growth in post-rift and contemporary, compressive-stress fields. In areas having young faults striking parallel to S3C veins, vein fibers in S2 fractures locally show complex, incremental rotations (Fig. 5a), mechanically-twinned calcite fibers (Fig. 5a) and shearing along fracture walls (Fig. 5c). Basin strata in these areas are cut, uplifted, and folded by late-stage, high-angle block faults (Herman, 2005a) forming positive flower structures (Harding, 1985). In eastern Pennsylvania, some Early Jurassic diabase dikes strike about E–W, cut Late Triassic strata and other dikes oriented along S2 directions, and align en échelon with late-stage, cross-strike, oblique-slip faults including the Chalfont fault (Fig. 1). The Chalfont strike bisects the S3C sector and cuts, offsets and folds Early Jurassic diabase (Berg et al., 1980).

6. Discussion

Based on the extension-fracture criteria outlined above, the mid-Atlantic continental margin in the Newark basin region involved Late Triassic to Early Jurassic rifting that later evolved into a third extension phase prior to the onset of regional compression. The timing and driving forces behind the shift from continental extension to compression is uncertain and the focus of continuing research and debate (see summaries and discussions by de Boer and Clifford, 1988; Schlische, 2003; among others). Appel and

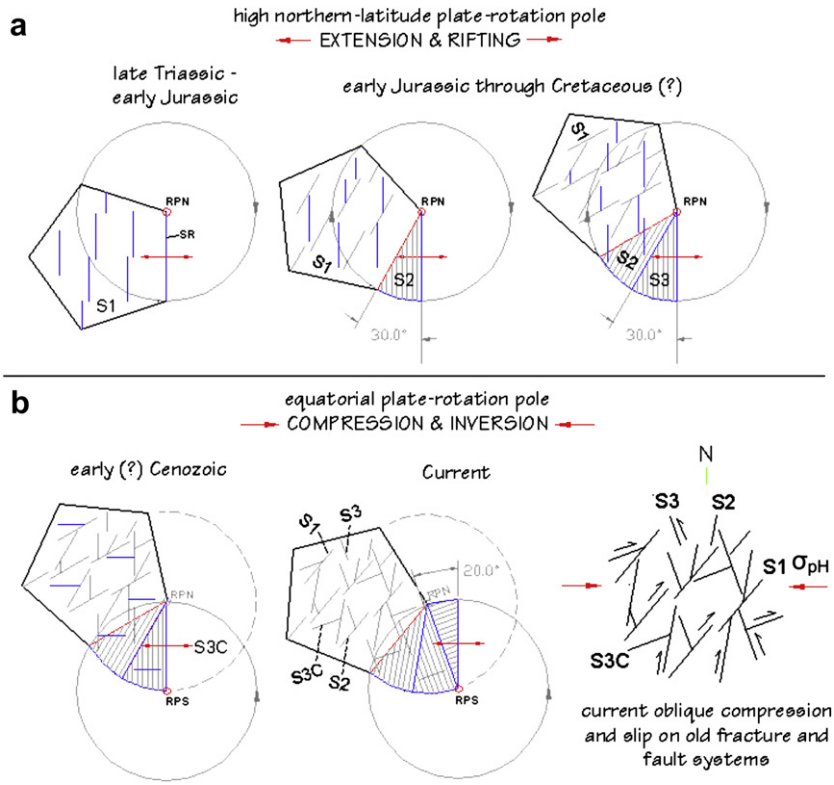

Fig. 19. Schematic interpretation of fracture-group formation and interactions with respect to a fixed spreading ridge (SR) and tectonic-plate rotations during the Mesozoic and Cenozoic Eras. Rifting and extension of the continental margin during the Mesozoic (a) resulted in three groups of extension fractures (S1–S3) formed within a tectonic plate rotating clockwise about an actual plate rotation pole located at high northern latitudes (RPN). Plate rotation changed polarity probably during the Early Cenozoic (b and Herman, 2006c) with a more southerly rotation pole (RPS), now located at equatorial latitudes (Drewes and Angermann, 2000). A change in rotation polarity may also have resulted in plate compression during the Cenozoic that is now directed about E–W (b) from ENE–WSW to WNW–ESE (Fig. 1). Latest-stage extension fractures (S3C) strike subparallel to contemporary, compressional plate stresses and about normal to latest rift-stage (S3) extension fractures. Current horizontal compression (σ_{pH}) could result in extension and opening of earlier S1 and S2 cross fractures and reactivated slip on rift-stage faults (b). S1 and S2 structures should now have a dextral-slip component but S3 structures should have a sinistral-slip component.

Fenster (1977) attributed oblique- to strike-slip reactivated motion on conjugate faults with S1 and S2 strikes as resulting from late compression directed normal to the continental margin and resulting in coeval slip on the conjugate systems. But as demonstrated above, S1–S3 extension fractures appear as having formed during separate tectonic episodes as part of a strain continuum involving incremental plate rotations within a tensional stress field. This latter scenario predicts oblique normal slip on progressively earlier S1–S3 fracture and fault groups during rifting stages until regional plate stress and rotation polarities changed. Current directions of principal horizontal compression in the region (σ_{pH} in Fig. 19) acting on preexisting S1–S3 extension planes would produce dextral-slip components on S1 and S2 planes but sinistral-slip components on pre-existing S3 planes (Fig. 19). More detailed fault-slip analyses using kinematic indicators such as small drag folds and slickensided shear planes are needed in order to confirm these relationships.

The plate rotations diagrammed in Fig. 19a outline a specific evolution of stretching episodes in the Newark basin since the Late Triassic. They show how plate rotation in one direction results in evolving, extensional strain fields in the opposite direction. The rotation values represent maximum values based on the fracture geometry and assuming a fixed plate rotation pole and spreading ridge. Actual plate rotations are less when poles and ridges vary in position and orientation through time, as during Mesozoic rifting and development of the Atlantic Ocean. Spreading-ridge jumps and shifts into new alignment during Juassic–Cretaceous opening of the north–central Atlantic region (Klitgord and Schouten, 1986) reflects continuous, northward-progressive opening of the ocean basin through the Mesozoic. Periodic shifts in position and alignment of opening centers involve large transform faults separating crustal blocks subject to different tensional stresses. Overall clockwise rotations of the North American plate (NAP) during the Mesozoic is supported by analyses of paleomagnetic Euler poles (Gordon et al., 1984; Butler, 1992) and plate-reconstruction models (Scotese and Sager, 1988; http://www.scotese.com/natlanim.htm). These same data and models also show counterclockwise rotation of the NAP during the Cenozoic and perhaps, a concomitant changes in NAP stresses from tension to compression. Current components of horizontal crustal compression (Fig. 1) are consistent with late-stage strain indicators in the Newark basin including the arrangements of basement-rooted, reverse- to oblique-slip block faults that modified earlier structures (Lucas et al., 1988; Schlische, 1992) and continue to reflect current plate motions and crustal seismicity (Herman, 2006c). These 'young' faults and folds probably link with other young structures extending beyond the basin into surrounding foreland and hinterland regions, including Cretaceous bedrock of the NJ Coastal Plain (Herman, 2005b). The precise age, map extent and geometry of these late-stage faults remain elusive but may involve anomalous fault systems mapped throughout the region during the past half century (Drake and Woodward, 1963; Woodward, 1964; Sheridan, 1976; Root and Hoskins, 1977; Sumner, 1978; Manspeizer and Cousminer, 1988; Hutchinson et al., 1986).

More work is needed to resolve the timing and driving mechanism behind NAP rotation-pole shifts and polarity reversals of plate motion. Also, indicators of current plate stresses need to be

reconciled with strain indicators relating episodes of basin inversion directed normal to the current structural grain of the NAP margin (Goldberg et al., 2003; Schlische, 2003) and N–S as determined by a calcite-twin strain analysis in the northern reaches of the basin (Lomando and Engelder, 1984) and late-stage thrust faults in the Hartford basin (Wise, 1988). Comparative studies of extension-fracture dynamics in Early Mesozoic basins along the NAP eastern margin should provide insight into more regional processes and tectonic strain fields.

Acknowledgements

I thank Irvin 'Butch' Grossman, Don Monteverde, Dave Hall, John Curran, Greg Steidl, Mike Serfes, 'Farmer Steve' Spayd and Karl Muessig of the NJ Geological Survey for their help, suggestions and reviews on various phases of this work. Part of this work was made possible by research grants obtained from the State of New Jersey, Department of Environmental Protection, Site Remediation Program as administered by Paul Sanders of the Division of Science and Research. Juliet Crider and Brian Wernicke provided constructive reviews of early versions of the manuscript. The latter's suggestion to tie the observed structural relationships to tectonic plate dynamics provided the impetus to expand the scope of the investigation to its current state. Don Wise provided a thoughtful review that helped clarify key points throughout the presentation. I especially thank Terry Engelder for his review and spearheading this volume in honor of Nick and Rick, who's mentoring and friendship I am very thankful for.

References

Appel, G., Fenster, D.F., 1977. Deformation of the northeast Newark basin. Geological Society of America Abstracts with Programs 9, 237.

Beach, A., 1975. The geometry of en-échelon vein arrays. Tectonophysics 28, 245–263.

Benson, R.N., 2002. Age estimates of the seaward dipping volcanic wedge, earliest oceanic crust, and earliest drift-stage sediments along the North American Atlantic continental margin. In: Hames, W.E., McHone, J.G., Renne, P.R., Ruppel, C. (Eds.), The Central Atlantic Magmatic Province. American Geophysical Union, Geophysical Monograph, vol. 136, pp. 61–76.

Berg, T.M., et al., 1980. Geologic map of Pennsylvania. Commonwealth of Pennsylvania Topographic and Geological Survey Map 1, 2 pl., scale 1.250,000.

Butler, R.F., 1992. Paleomagnetism: Magnetic Domains to Geologic Terranes. Blackwell Scientific Publications, Boston, MA, 319 pp.

de Boer, J.Z., Clifford, A.E., 1988. Mesozoic tectogenesis. Development and deformation of 'Newark' rift zones in the Appalachian (with special emphasis on the Hartford basin, Connecticut). In: Manspeizer, W. (Ed.), Triassic–Jurassic Rifting, Continental Breakup, and the Origin of the Atlantic Ocean and Passive Margin. Elsevier, New York, pp. 275–306 (Chapter 11).

Drake, C.L., Woodward, H.P., 1963. Appalachian curvature, wrench faulting, and offshore structures. New York Academy of Science Transactions Series 2 (26), 48–63.

Drewes, H., Angermann, D., 2000. The Actual Plate Kinematic and Crustal Deformation Model 2000 (APKIM2000) as a Geodetic Reference System. AIG 2001 Scientific Assembly, Budapest, 2–8 Sept 2001. Available from the Internet World-Wide-Web at http://dgfi2.dgfi.badw-muenchen.de/dgfi/DOC/2001/DS_APKIM.pdf.

Dula, W.F., 1991. Geometric models of listric normal faults and rollover folds. American Association of Petroleum Geologists Bulletin 75 (10), 1609–1625.

Dunning, G.R., Hodych, J.D., 1990. U-Pb zircon and baddeleyite age for the Palisade and Gettysburg sills of northeast United States. Implications for the age of the Triassic–Jurassic boundary. Geology 18, 795–798.

Durney, D.W., Ramsay, J.G., 1973. Incremental strains measured by syntectonic crystal growths. In: DeJong, K.A., Scholten, R. (Eds.), Gravity and Tectonics. Wiley-Interscience, New York, pp. 67–96.

El Tabakh, M., Schreiber, B.C., 1998. Diagenesis of the Newark rift basin, eastern. North America. Sedimentology 45, 855–874.

El Tabakh, M.E., Riccioni, R., Schreiber, B.C., 1997. Evolution of late Triassic rift basin evaporites (Passaic Formation), Newark basin, eastern North America. Sedimentology 44, 767–790.

El Tabakh, M.E., Schreiber, B.C., Warren, J.K., 1998. Origin of fibrous gypsum in the Newark rift basin, eastern North America. Journal of Sedimentary Research 68, 88–99.

Engelder, T., 1997. Transitional-tensile fracture propagation: a status report. Journal of Structural Geology 21, 1049–1055.

Faust, G.T., 1978. Joint Systems in the Watchung Basalt Flows. U.S. Geological Survey Professional Paper 864-B, New Jersey, 46 p.

Goldberg, D., Lupo, T., Caputi, M., Barton, C., Seeber, L., 2003. Stress regimes in the Newark basin rift: evidence from core and downhole data. In: LeTourneau, M., Olsen, P.E. (Eds.), The Great Rift Valleys of Pangea in Eastern North America 1, Tectonics, Structure, and Volcanism. Columbia University Press, New York (Chapter 7).

Gordon, R.G., Cox, A., O'Hare, S., 1984. Paleomagnetic Euler poles and the apparent polar wander and absolute motion of North America since the Carboniferous. Tectonics 3, 499–537.

Groshong, R.H., 1988. Low-temperature deformation mechanisms and their interpretation. Geological Society of America Bulletin 100, 1329–1360.

Gross, M.R., 1993. The origin and spacing of cross joints, examples from the Monterey Formation, Santa Barbara Coastline, California. Journal of Structural Geology 15, 737–751.

Harding, T., 1985. Seismic characteristics and identification of negative flower structures, positive flower structures, and positive structural inversion. American Association of Petroleum Geologists Bulletin 69, 582–600.

Herman, G.C., 1997. Digital mapping of fractures in the Mesozoic Newark basin, New Jersey: developing a geological framework for interpreting movement of groundwater contaminants. Environmental Geosciences 4, 68–84.

Herman, G.C., 2001. Hydrogeological framework of bedrock aquifers in the Newark Basin, New Jersey. In: LaCombe, P.J., Herman, G.C. (Eds.), Geology in Service to Public Health. Eighteenth Annual Meeting of the Geological Association of New Jersey, South Brunswick, N.J., pp. 6–45.

Herman, G.C., 2005a. Joints and veins in the Newark basin, New Jersey, in regional tectonic perspective. In: Gates, A.E. (Ed.), Newark Basin – View from the 21st Century, 22nd Annual Meeting of the Geological Association of New Jersey, College of New Jersey, Ewing, New Jersey, pp. 75–116.

Herman, G.C., 2005b. STOP 3: Stratigraphy and structure of the Passaic Formation and Orange Mt. Basalt at Mine Brook Park, Flemington, New Jersey. In: Gates, A.E. (Ed.), Newark Basin – View from the 21st Century, 22nd Annual Meeting of the Geological Association of New Jersey, College of New Jersey, Ewing, New Jersey, pp. 134–144.

Herman, G.C., 2006a. Hydrogeological framework of the Brunswick aquifer at Heron Glen Golf Course, Hunterdon County, New Jersey. NJ Geological Survey Newsletter 2, 8–11.

Herman, G.C., 2006b. Hydrogeological framework of Middle Proterozoic granite and gneiss from borehole geophysical surveys at two ground-water pollution sites, Morris County, NJ. In: Macaoay, S., Montgomery, W. (Eds.), Environmental Geology of the Highlands, 23rd Annual Meeting of the Geological Association of New Jersey. Ramapo College of New Jersey, Mahwah, New Jersey, pp. 26–45.

Herman, G.C., 2006c. Neotectonic setting of the North American Plate in relation to the Chicxulub impact. Geological Society America Abstracts with Programs 38, 415.

Hodgson, R.A., 1961. Regional study of jointing in Comb ridge-Navajo Mountain Area, Arizona and Utah. American Association of Petroleum Geologists Bulletin 45, 1–38.

Huang, Q., Angelier, J., 1989. Fracture spacing and its relation to bed thickness. Geological Magazine 126, 355–362.

Hutchinson, D.R., Klitgord, K.D., 1988. Evolution of rift basins on the continental margin of southern New England. In: Manspeizer, W. (Ed.), Triassic–Jurassic Rifting, Continental Breakup, and the Origin of the Atlantic Ocean and Passive Margin. Elsevier, New York, NY, pp. 82–97 (Chapter 4).

Hutchinson, D.R., Klitgord, K.D., Detrick, R.S., 1986. Rift basins of the Long Island platform. Geological Society of America Bulletin 97, 688–702.

Jet Propulsion Laboratory, 2008. Global Positioning System (GPS) time series data, California Institute of Technology under contact with the National Aeronautics and Space Administration. Available from the Internet World-Wide-Web at http://sideshow.jpl.nasa.gov/mbh/series.html.

Klitgord, K.D., Schouten, H., 1986. Plate kinematics of the central Atlantic. In: Vogt, P.R., Tucholke, B.E. (Eds.), The Geology of North America, The Western North Atlantic Region. Geological Society of America DNAG M, pp. 351–378.

Laney, S.E., Husch, J.M., Coffee, C., 1995. The petrology, geochemistry and structural analysis of late-stage dikes and veins in the Lambertville sill, Belle Mead, New Jersey. Northeastern Geology and Environmental Sciences 17, 130–145.

Lindholm, R.C., 1978. Triassic–Jurassic faulting in eastern North America – a model based on pre-Triassic structures. Geology 6, 365–368.

Lomando, A.J., Engelder, T., 1984. Strain indicated by calcite twinning: implications for deformation of the early Mesozoic northern Newark basin, New York. Northeast Geology 6, 192–195.

Lucas, M., Hull, J., Manspeizer, W., 1988. A foreland-type fold and related structures of the Newark rift basin. In: Manspeizer, W. (Ed.), Triassic–Jurassic Rifting, Continental Breakup, and the Origin of the Atlantic Ocean and Passive Margin. Elsevier, New York, NY, pp. 307–332 (Chapter 12).

Manspeizer, W., Cousminer, H.L., 1988. Late Triassic–Early Jurassic synrift basins of the U.S. Atlantic margin. In: Sheridan, R.E., Grow, J.A. (Eds.), The Geology of North America, The Atlantic Continental Margin, U.S.A. Geological Society of America I-2, pp. 197–216.

McClay, K., Bonora, M., 2001. Analog models of retraining stepovers in strike-slip fault systems. American Association of Petroleum Geologists Bulletin 85 (2), 233–260.

Merguerian, C., Sanders, J.E., 1994. Implications of the Graniteville xenolith for flow directions of the Palisades magma. In: Benimoff, A.I. (Ed.), The Geology of Staten Island, New York. Eleventh Annual Meeting of the Geological Association of New Jersey, Somerset, NJ, p. 59.

Monteverde, D.H., Volkert, R.A., 2005. Bedrock Geologic Map of the Chatham Quadrangle, Morris, Somerset and Union Counties, New Jersey. NJ Geological Survey Geologic Map Series GMS 04-2, scale: 1:24,000.
Monteverde, D.H., Stanford, S.D., Volkert, R.A., 2003. Geologic Map of the Raritan Quadrangle, Hunterdon and Somerset Counties, New Jersey. N.J. Geological Survey Geologic Map Series GMS 03-2, scale 1:24,000.
Narr, W., Suppe, J., 1991. Joint spacing in sedimentary rocks. Journal of Structural Geology 13, 1037–1048.
New Jersey Geological Survey, 2000, Bedrock Geology and Topographic Base Maps of New Jersey, 1.100,000 scale, New Jersey Geological Survey Compact Disc Series CD-01.
Nicholson, R., Pollard, D.D., 1985. Dilation and linkage of échelon cracks. Journal of Structural Geology 7, 583–590.
Olsen, P.E., Withjack, M.O., Schlische, R.W., 1992. Inversion as an integral part of rifting. An outcrop perspective from the Fundy basin, eastern North America. Eos—American Geophysical Union Transactions 73, 562.
Olsen, P.E., Kent, D., Cornet, B., Witte, W.K., Schlische, R.W., 1996a. High-resolution stratigraphy of the Newark rift basin (early Mesozoic, eastern North America). Geological Society of America Bulletin 108, 40–77.
Olsen, P.E., Schlische, R.W., Fedosh, M.S., 1996b. 580 Ky Duration of the Early Jurassic flood basalt event in eastern North America estimated using Milankovitch Cyclostratigraphy. In: Morales, M. (Ed.), The Continental Jurassic. Museum of Northern Arizona Bulletin, vol. 60, pp. 11–22.
Parnell, J., Monson, B., 1995. Paragenesis of hydrocarbon, metalliferous and other fluids in Newark Group basins, Eastern U.S.A., Institute of Mining and Metallurgy. Transactions, Section B. Applied Earth Science 104 136-144.
Pollard, D.P., Aydin, A., 1988. Progress in understanding jointing over the past century. Geological Society of America Bulletin 100 1181–1024.
Ramsay, J.G., 1980. The crack-seal mechanism of rock deformation. Nature 284, 135–139.
Ramsay, J.G., Huber, M.I., 1983. The Techniques of Modern Structural Geology 1. Strain Analysis. Academic Press, London, UK, p. 307.
Ratcliffe, N.M., Burton, W.C., 1985. Fault reactivation models for the origin of the Newark basin and studies related to U.S. eastern seismicity. U.S. Geological Survey Circular 946, 36–45.
Root, S.I., Hoskins, D.M., 1977. Lat 40°N fault zone, Pennsylvania. A new interpretation. Geology 5, 719–723.
Sanders, J.E., 1963. Late Triassic tectonic history of Northeastern United States. American Journal of Science 261, 501–524.
Schlische, R.W., 1992. Structural and stratigraphic development of the Newark extensional basin, eastern North America. Evidence for the growth of the basin and its bounding structures. Geological Society of America Bulletin 104, 1246–1263.
Schlische, R.W., 1993. Anatomy and evolution of the Triassic–Jurassic continental rift system, eastern North America. Tectonics 12, 1026–1042.
Schlische, R.W., 2003. Progress in understanding the structural geology, basin evolution, and tectonic history of the eastern North American rift system. In: LeTourneau, P.M., Olsen, P.E. (Eds.), The Great Rift Valleys of Pangea in Eastern North America 1, Tectonics, Structure, and Volcanism. Columbia University Press, New York, pp. 21–64.
Schlische, R.W., Olsen, P.E., 1988. Structural evolution of the Newark Basin. In: Husch, J.M., Hozik, M.J. (Eds.), Geology of the Central Newark BasinField Guide and Proceedings: 5th Annual Meeting of the Geological Association of New Jersey. Rider College, Lawrenceville, NJ, pp. 43–65.
Schlische, R.W., Withjack, M.O., Eisenstadt, G., 2002. An experimental study of secondary deformation produced by oblique-slip normal faulting. American Association of Petroleum Geologists Bulletin 86, 885–906.
Scotese, C.R., Sager, W.W., 1988. Mesozoic and Cenozoic plate tectonic reconstructions. Tectonophysics 155, 27–48.
Sheridan, R.E., 1976. Conceptual model for the block-fault origin of the North American Atlantic continental margin geosyncline. Geology 2, 465–468.
Simonson, B.M., Smoot, J.P., 1994. Distribution and origin of macropore-filling cements in nonmarine mudstones, early Mesozoic Newark Basin, New Jersey and Pennsylvania. Geological Society of America, Abstracts with Programs 26, 337.
Smoot, J.P., Olsen, E., 1994. Climatic cycles as sedimentary controls of rift-basin lacustrine deposits in the early Mesozoic Newark Basin based on continuous core. In: Lomando, T., Harris, M. (Eds.), Lacustrine Depositional Systems. Society of Sedimentary Geology (SEPM) Core Workshop Notes, vol. 19, pp. 201–237.
Smoot, J., Simonson, B.M. 1994. Alkaline authigenic minerals in the early Mesozoic Newark Basin, NY, NJ, PA; evidence for late fluid movement through mudstones. American Association of Petroleum Geologists and Society of Economic Paleontologists and Mineralogists 1994, 261–262.
Stanford, S.D., Monteverde, D.H., Volkert, R.A., 1998. Geology of the New Brunswick Quadrangle, Middlesex and Somerset Counties, New Jersey, N.J. Geological Survey Open-file Map OFM 23, scale 1:24,000.
Steckler, M.S., Omar, G.I., Karmer, G.D., Kohn, B.P., 1993. Pattern of hydrothermal circulation within the Newark basin from fission-track analysis. Geology 21, 735–738.
Sumner, J.R., 1978. Geophysical investigation of the structural framework of the Newark–Gettysburg Triassic basin, Pennsylvania. Geological Society of America Bulletin 88, 935–942.
Sutter, J.F., 1988. Innovative approaches to the dating of igneous events in the early Mesozoic basins of the eastern United States. In: Froelich, A.J., Robinson Jr., G.R. (Eds.), Studies of the Early Mesozoic Basins of the Eastern United States. U.S. Geological Survey Bulletin, vol. 1776, pp. 194–200.
Swanson, M.T., 1986. Preexisting fault control for Mesozoic basin formation in eastern North America. Geology 14, 419–422.
Van de Kamp, C., Leake, B.E., 1996. Petrology, geochemistry, and Na metasomatism of Triassic–Jurassic non-marine clastic sediments in the Newark, Hartford, and Deerfield rift basins, northeastern USA. Chemical Geology 133, 89–124.
Van der Pluijm, B.A., Marshak, S., 1997. Earth Structure: An Introduction to Structural Geology and Tectonics. McGraw-Hill, New York.
Van Houten, F.B., 1964. Crystal casts in upper Triassic Lockatong and Brunswick Formations. Sedimentology 4, 301–313.
Van Houten, F.B., 1965. Composition of Triassic Lockatong and associated formations of Newark Group, central New Jersey and adjacent Pennsylvania. American Journal of Science 263, 825–863.
Volkert, R.A., 2006a. BedrockGeologic Map of the Caldwell Quadrangle, Essex and Morris Counties, New Jersey: NJGS Geologic Map Series GMS 06-3, scale 1:24,000.
Volkert, R.A., 2006b. Bedrock Geologic Map of the Paterson Quadrangle, Passaic, Essex and Bergen Counties: N.J. Geological Survey Geologic Map Series GMS 06-6, scale 1:24,000.
Wise, D.U., 1988. Mesozoic stress history of the upper Connecticut Valley at Turners Falls, Massachusetts. In: Bothner, W.A. (Ed.), Guidebook for Field Trips in Southwestern New Hampshire, Southeastern Vermont, and North-Central Massachusetts. New England Intercollegiate Geological Conference, 74th Annual Meeting, Keene, NH, Field Trip C- 7, pp. 351–372.
Withjack, M.O., Islam, Q.T., La Pointe, R., 1995. Normal faults and their hanging-wall deformation: an experimental study. American Association of Petroleum Geologists Bulletin 79 (1), 1–18.
Withjack, M.O., Schlische, R.W., Olsen, E., 1998. Diachronous rifting, drifting, and inversion on the passive margin of eastern North America: an analogue for other passive margins. American Association of Petroleum Geologists Bulletin 82, 817–835.
Woodward, H.P., 1964. Central Appalachian tectonics and the deep basin. American Association of Petroleum Geologists Bulletin 48, 338–356.
Xiao, H., Suppe, J., 1992. Origin of rollover. American Association of Petroleum Geologists Bulletin 76, 509–529.
Younes, A.L., Engelder, T., 1999. Key structures for the interpretation of the progressive Alleghanian deformation of the Appalachian Plateau. Geological Society of America Bulletin 111, 219–239.